# De novo fabrication of oral insulin-loaded chitosan/dextrin/pectin nanospheres and their antidiabetic efficacy in streptozotocin-induced diabetic rats

S. R. Mohammed[a], A. Abdel-Moneim[a], E. S. Abdel-Reheim[a], H. Ramadan[b], Z. E. Eldin[c], A. A. G. El-Shahawy[c], A. I. Yousef[a,*]

[a]*Molecular Physiology Division, Zoology Department, Faculty of Science, Beni-Suef University, Egypt*

[b]*Cell Biology, Histology and Genetics Division, Zoology Department, Faculty of Science, Beni-Suef University, Egypt*

[c]*Materials Science and Nanotechnology Department, Faculty of Postgraduate Studies for Advanced Sciences (PSAS), Beni-Suef University, Egypt*

Nanotechnology can offer various non-invasive and efficient alternative delivery strategies for insulin injections to enhance the quality of life of diabetic patients. The current research was aimed to fabricate a de novo oral formula of insulin-loaded chitosan nanoparticles coated with dextrin and pectin (INS-CN/DP) to improve the bioavailability and therapeutic efficiency of oral insulin. INS-CN/DP nano-formula was prepared using ionic gelation technique and characterized by XRD, FTIR, SEM, EDX, and DLS. Insulin loading capacity and entrapment efficiency (LC%, EE%), release profile, and kinetic study was conducted for INS-CN/DP nano-formula. Next, hypoglycemic and antidiabetic efficiency of INS-CN/DP nano-formula were studied in streptozotocin-induced diabetic rats by measuring fasting and postprandial glucose, the activities of carbohydrate metabolizing enzymes, liver glycogen content, and gene expression levels of glucokinase and Glucose transporter-2. Characterization results confirmed the formation of INS-CN/DP nanoparticles with LC% =26.2 ± 0.56 and EE% 69.3 ± 2.75, respectively. Size average was 282.8 nm and nearly 25% of loaded insulin released after 4 hrs vs 48% for unloaded insulin. *In vivo* results displayed that oral administration of INS-CN/DP nanoparticles showed highly significant hypoglycemic and antidiabetic efficacy in diabetic rats compared to unloaded oral insulin. Oral INS-CN/DP nano-formula is promising alternative for insulin injections and can be suggested as non-invasive and effective diabetes therapy.

(Received November 21, 2023; Accepted April 2, 2024)

*Keywords:* Oral insulin, Chitosan nanospheres, Characterization, Anti-diabetic efficacy

## 1. Introduction

Basically, subcutaneous insulin delivery is the most effective treatment for diabetic patients. However, this method of insulin administration has various limitations, such as infection, insulin precipitation, and either lipo-hypertrophy or lipo-atrophy at the injection site. Also, it is painful and inconvenient because most patients need to inject themselves at least two times per day during their lives [1], [2]. Recently, many alternative strategies of non-invasive insulin delivery based on nanotechnology have been developed, including oral, nasal, ocular, buccal, pulmonary, and transdermal routes [3]. This generation of new non-invasive and efficient insulin nano-therapies can help to enhance the quality of life of diabetic patients.

The oral route for insulin delivery is very convenient for diabetics; however, many challenges have to be ignored, such as loss of insulin in the gastrointestinal tract (GIT) and little oral bioavailability [4]. It is reported that the bioavailability of orally administered insulin is less than 10% [5]. Insulin encapsulation within nanocarriers enhances the bioavailability and efficiency of oral insulin, which could be attributed to 1) inhibiting degradation by digestive enzymes in the GIT; 2) increasing the stability of poorly soluble insulin; 3) enhancing the effectiveness of drug

* Corresponding author: ahmedyousef@science.bsu.edu.eg
https://doi.org/10.15251/JOBM.2024.162.73

delivery at the site of absorption; and 4) prolonging drug release properties [6]. For example, treatment of diabetic rats with oral insulin-loaded chitosan nanoparticles (21 IU/kg) produced hypoglycemic action that extended up to 15 h with an average pharmacological bioavailability of about 14.9% compared to subcutaneous injection [7].

Nanocarriers could be developed from natural or synthetic polymers. Natural hydrophilic polymers like chitosan, pectin, and dextrin have various promising properties, including safety, biocompatibility, and biodegradability [8]. At the same time, nanocarrier-forming polymers can display many beneficial biological effects. The consumption of chitosan oligosaccharide can effectively reduce postprandial blood glucose levels [9]. Chitosan showed to raise the lipolysis rate; decreased hepatic enzyme activities of lipid biosynthesis downregulates the expression of lipogenesis-associated genes (FAS and HMGCR) in hepatocytes [10]. A high-pectin diet has been suggested to be effective for diabetes management. Several studies have shown the positive effect of pectin on the reduction of blood glucose. Liu *et al.* [11] reported that the anti-diabetic action of citrus pectin may be explained by modulation of the PI3K/Akt signalling pathway. Dextrin has also been shown to decrease triglyceride levels and reduce the glycemic index of meals, which helps to maintain healthy blood sugar levels [12]. Furthermore, dextran can protect insulin against the GIT proteases via its chemical linkage to insulin [13].

Considering the foregoing, the present study was aimed to develop a de novo oral formula of insulin-loaded chitosan nanoparticles coated with dextrin and pectin (INS-CN/DP) to improve the bioavailability and therapeutic efficiency of oral insulin. Therefore, an insulin nano-formula was prepared, characterized, and investigated for its antidiabetic efficacy in diabetic rat model.

## 2. Materials and methods

### 2.1. Chemicals

Streptozotocin, sodium tripolyphosphate, and dextran were purchased from Sigma Aldrich Co., MO, USA. Insulin (Insulatard®) was obtained from Novo Nordisk Co., Copenhagen, Denmark. Chitosan with medium MW (average molecular weight, 200 kDa) was purchased from Techno Pharmchem Co., Delhi, India. Sodium hydroxide and glacial acetic acid were obtained from Loba Chemie, Mumbai, India. Pectin was purchased from Nakaa nanotechnology company, Cario, Egypt. All other supplies were of analytical grade and were obtained from standard commercial sources.

### 2.2. Synthesis of INS-CN/DP Nanoparticles

INS-CN/DP nanoparticles were prepared according to a modified ionic gelation method [14]. The concentration of chitosan (0.3%, w/v) in DW containing 1% acetic acid, pH 4.8, and the chitosan/sodium tripolyphosphate (TPP) ratio of 4:1 was adjusted. Nanoparticles were obtained after addition of TPP solution (dropwise) to chitosan solution under magnetic stirring using stirrer for 30 min at 1000 Rpm. Then 0.1g of dextrin was dissolved in 10 mL of deionized water (1.0% w/v) and gelatinized in a boiling water bath then cooled to room temperature. 500 ug/ml of insulin was added drop by drop to the previous solution, stirred magnetically at 1000 r/min for 1 h, then dextrin insulin solution was added to the above solution [15]. Then the pectin was added (4% w/v) using a high-speed homogenizer to the above solution (chitosan, dextrin, and insulin) and then stored at 4 °C for 48 h [16]. Next, the solution was centrifuged to obtain the precipitates.

### 2.3. Characterizations

#### *2.3.1. X-ray Diffraction (XRD) and Fourier Transformation Infrared Spectroscopy (FTIR)*

The XRD technique was performed to investigate the crystallinity of the prepared samples using Cu K α radiation (λ = 1.54 Å). The instrument (PANalytical Empyrean) was run at an operating voltage of 40 kV with a power of 1200 W and current of 30 mA. Scans were recorded from 10° to 70° 2θ at a speed of 2°/min with a step size of 0.050° and step time of 1.5 seconds.

FTIR spectra was carried out using a Bruker (Vertex 70 FTIR-FT Raman) spectrometer to determine the functional groups. Pellets of 10.0 mm and 1-2 mm thickness were prepared from

samples mixed with potassium bromide (KBr) and compressed under high pressure then scanned within a range from 500 to 4000 $cm^{-1}$.

### *2.3.2. Morphology Study and The Elemental Analysis*

Field emission scanning electron microscopy (FESEM) using a Philips-XL30 instrument was performed to examine the particle size, surface morphology and elemental composition of the formulated INS-CN/DP nanoparticles. The FESEM was equipped with energy dispersive X-ray (EDX) spectroscopy for elemental analysis. Samples were prepared by dispersing the nanoparticles in deionized water followed by 1:5 dilution at room temperature.

### *2.3.3. Zetasizer and Zeta Potential Measurements*

Dynamic light scattering (DLS) using a Malvern Zetasizer ZS90 instrument (Malvern, UK) was utilized to determine the particle size distribution, mean hydrodynamic diameter, and polydispersity index of the dispersed INS-CN/DP nanoparticles. DLS measures the intensity fluctuations in scattered light caused by the Brownian motion of nanoparticles to obtain size and distribution. Electrophoretic laser Doppler velocimetry on the same instrument was used to estimate the zeta potential, which indicates the surface charge and colloidal stability. Samples were prepared by sonicating 5 mL of INS-CN/DP nanoparticles for 90 s at 40 W power before transfer for analysis.

### *2.3.4. Loading Capacity and Entrapment Efficiency*

To determine the loading capacity (LC%) and encapsulation efficiency (EE%) of insulin in the nano-formulation, the nanoparticles were centrifuged at 14,000 rpm and 4°C for 45 minutes. This separated the supernatant containing unencapsulated free insulin. The concentration of free insulin in the supernatant was then quantified by UV-Vis spectrophotometry at λmax= 276 nm. All measurements were performed in triplicates (n=3). The loading capacity percent (% LC) of the formula and the insulin entrapment efficiency (EE%) were calculated according to Ghosheh *et al.* [17] as follows:

$$\mathrm{LC\%} = \frac{(Initial\ insulin - free\ insulin)}{Formula}\, x\ 100 \tag{1}$$

$$\boldsymbol{EE\%} = \frac{\boldsymbol{(Total\ amount\ of\ Ins - free\ amount\ of\ Ins)}}{\boldsymbol{Total\ amount\ of\ Ins}}\, x100 \tag{2}$$

### *2.3.5. In Vitro Insulin Release Study*

The sustained release profile of insulin from the prepared INS-CN/DP nanoparticles was evaluated using a modified dialysis bag technique [18]. Briefly, 5 mL of insulin solution and nanoparticles suspension (equivalent to 20 mg insulin) were placed in separate dialysis bags (cellophane, 10-12 kDa cutoff). Bags were sealed and immersed in 200 mL phosphate buffer (pH 7.4) at 37°C.The bags were kept in a shaking incubator at 37°C and 150 rpm. At intervals, 1.5 mL was withdrawn from the release medium and centrifuged at 13,000 rpm for 15 mins. The supernatant (1 mL) containing released insulin was mixed with 2 mL ethanol. The absorbance was measured at 276 nm by UV-vis spectrophotometry. The cumulative amount of insulin released at each time point was calculated as a percentage of initial loaded insulin. Measurements were made in triplicates.

### *2.3.6. Kinetics Release of Insulin from INS-CN/DP Nanoparticles*

The *in vitro* insulin release data was fitted to various kinetic models including zero-order, first-order, Hixson-Crowell, Korsmeyer-Peppas and Higuchi to analyze the release mechanism. The correlation coefficient ($R^2$) values indicated the best fit model. The Peppas equation was applied to determine the release mechanism [19]:

$$\frac{M_t}{M_\infty} = \mathrm{K}t^n \quad (3)$$

where, Mt is the amount of drug released at time t.

M∞ is the total amount released at infinite time.

K is the release rate constant.

n is the diffusion exponent of Peppas.

**2.4. Animals**

The current investigation used adult male albino rats (Rattus norvegicus) weighing around 120± 10g and having an age of 10± 2 weeks were incorporated. These animals were obtained from the Holding Company for Biological Products and Vaccines (VACSERA, Cairo, Egypt). Rats were housed one week under non-stressful standard conditions (temperature: 25± 5 °C, humidity: 55 ± 5%, and light-dark cycle: 12:12 h) for adaptation and supplied with water and a normal basal diet with known composition ad libitum during the experimental period. All animal experiments were approved and conducted according to the guidelines of the Institutional Animal Care and use Committee (IACUC) of Beni-Suef University (BSU-IACUC Approval Number: 021-131).

**2.5. Induction of Diabetes Mellitus in Rats**

Experimental diabetes mellitus was established by a single dose of streptozotocin (55 mg STZ/kg b.w.t., Immediately dissolved in cold citrate buffer, pH 4.5) was administered intraperitoneally by injection in overnight-fasted rats [20]. Seven days later, fasting blood glucose level was measured; rats with a fasting blood glucose ≥ 200 mg/dl were considered stable mild diabetics and included in the herein experiments.

**2.6. Administration of INS-CN/DP Nanoparticles to Rats**

Rats were classified into the five groups (n = 6) as follows: normal control rats (Ctrl) received vehicle; diabetes mellitus control rats (DM) received vehicle; diabetic rats treated with unloaded insulin (DM+INS, 50 IU/kg b.wt.); diabetic rats treated with INS-CN/DP nanoparticles (DM+INS-CN/DP, 50 IU/kg b.wt.); and diabetic rats treated with an equivalent amount of blank CN/DP nanoparticles (DM+CN/DP) corresponding to those in 50 IU/kg of INS-CN/DP nanoparticles. All treatments were administered daily for one month via oral gavage. The doses were adjusted every week based on the body weight.

**2.7. Biological examinations**

***2.7.1. Determination of the Blood Glucose Levels***

Fasting blood glucose levels in experimental groups were measured in samples gathered from the lateral tail vein of fasted rats (8–10 hours) at the end of experiment by the CERA-CHECKTM 1070 glucometer (maximum measuring capacity of 600 mg/dL). Next, postprandial blood glucose levels (2 hours) were performed for all groups in response to glucose intake (3 g/kg b.w.t.) through gastric intubation.

***2.7.2. Determination of the Activities of Carbohydrate Metabolizing Enzymes and Liver Glycogen Content***

The activity changes of serum succinate dehydrogenase, pyruvate kinase, and glucose-6-phosphate dehydrogenase were assayed by an ELISA reagent kit purchased from BioVision Incorporated (Milpitas, USA), Bio Matik Incorporated (Cambridge, Canada), and Abbexa International (Houston, USA), respectively, according to the manufacturer's instructions. Liver glycogen content was assayed by an ELISA reagent kit purchased from My BioSource (California, USA) according to the manufacturer's instructions.

### *2.7.3. Determination the Gene Expression Levels of GK And GLUT2 by Quantitative Real Time PCR (qRT-PCR)*

RNA was extracted from the liver using a nucleic acid extraction kit (NucleoSpin® REF. 740901.250) purchased from Macherey-Nagel GmbH & Co. KG, Germany. The RNA purity (A260/A280 ratio) and concentration were acquired using spectrophotometry (dual-wavelength Beckman spectrophotometer, USA). The extracted and purified DNA samples were stored at -80 °C for further use.

qRT-PCR amplification and analysis were performed using the kit provided by Bioline, a median life science company in the UK (SensiFASTTM SYBR® Hi-ROX One-Step Kit, PI-50217 V). The following primer pairs were used: For GK, the forward primer sequence was 5′TCAACTACAGAAAATGGCGGAA 3′ and the reverse one was 5′ CCAGAACTGTAAGCCACTCG 3′; for GLUT2, the forward primer sequence was 5′-TCAACTACAGAAAATGGCGGAA 3′ and the reverse one was 5′ CCAGAACTGTAAGCCACTCG 3′; for GAPDH, the forward primer sequence was 5′-ATTCAACGGCACAGTCAA 3′ and the reverse one was 5′ CTTCTGGGTGAT 3′. The relative quantification was calculated according to Applied Biosline software using the ΔΔ Ct method. The mRNA expression levels of each gene were normalized to those of GAPDH.

### 2.8. Statistical analysis

The collected data were presented as mean ± standard error (SEM). Data was subjected to One-Way Analysis of Variance (ANOVA) using a computer software package (SPSS version 20, IBM Corp., 2011), and followed by the least significant difference multiple comparisons test to determine the significant differences between groups, at $P < 0.05$.

## 3. Results and discussion

### 3.1. Interpretation of XRD, FTIR, SEM, and EDX results

As illustrated in Fig. 1, The crystallinity of prepared samples (CHSNPs and INS-CN/DP nanoparticles) and raw materials (Dextrin and Pectin) was investigated by XRD analysis. The diffraction peaks of the CHSNPs showed a characteristically wide peak at 21.2° due to their highly amorphous nature. Dextrin presented a broad hump between (2) 14.8° and 27.2°, corresponding to its amorphous nature. The XRD pattern of pectin showed the characteristic sharp crystallization peak at 14.3°, 25.5°, 32.8°, and 39°, respectively. In the XRD pattern of INS-CN/DP nano-formula, the distinctive diffraction peaks of Pectin and dextrin disappeared. The formula showed the characteristic broad peak of CHS NPs nearly at 22°, indicating the proper interaction between CHS, dextrin, pectin, and insulin [21].

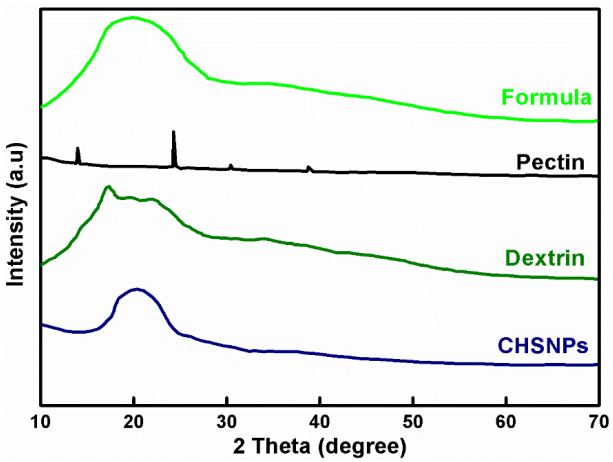


*Fig. 1. XRD of CHS, CHSNPs, Dextrin, Pectin, and INS-CN/DP nano-formula.*

Fig. 2 displays the FTIR spectra of CHS and CHSNPs. The spectra were similar with slight variations in peak broadness and positions, indicating successful nanoparticle formation. For CHS, the broad peak at 3420 cm−1 corresponds to overlapping O-H and N-H stretches. Peak broadening in CHSNPs suggests hydrogen bond formation [22]. The FTIR spectrum of dextrin is shown in the same figure. Dextrin spectrum showed characteristics bands at 3450 and 2970 cm-1 representing O-H and C-H stretches respectively. Fingerprint region peaks at 1030, 1267, 1153 cm-1 are distinctive of dextrin. Bands at 940 and 760 cm−1 indicate ring vibrations of glycosidic linkages [23]. Pectin exhibited typical peaks at 1610 cm-1 for COO- asymmetric stretch and 1745 cm-1 for COOH/COOCH3 groups [24]. Range 1200-950 cm-1 represents carbohydrate fingerprint region [25]. INS-CN/DP nano-formulation spectrum revealed specific peaks of individual components with slight broadening/shifting, indicating preservation of chemical integrity and interactions like hydrogen bonding during loading.

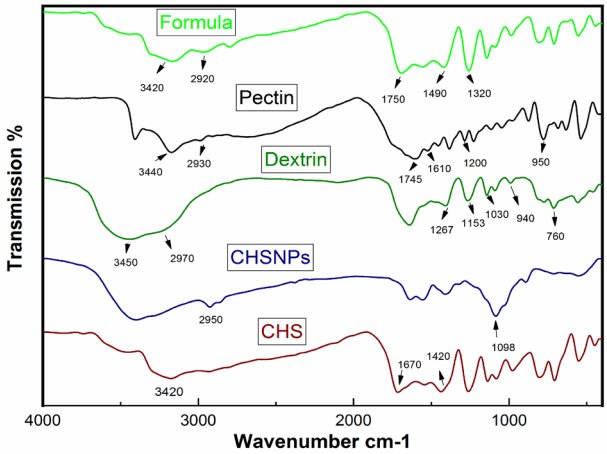


*Fig. 2. FTIR of CHS, CHSNPs, Dextrin, Pectin, and INS-CN/DP nano-formula. The peak patterns and positions of the formula varied significantly; these variations reflected interaction between entities, confirming the loading process.*

The SEM was employed to study the surface of the prepared INS-CN/DP nano-formula (Fig. 3a). The SEM image revealed a complex network of CHSNPs with wide pores (red circle) and surface discontinuities. Furthermore, the image of CHSNPs indicated irregularity and roughness in the surface texture with straps and shrinkage (blue arrows). Also, the SEM displayed aggregated particles with irregular morphology and a snow-white signal intensity. The irregular particle morphology could be related to the presence of surface-active functional groups in pectin, dextrin, and the terminal carboxylic and amino groups of the amino acids of insulin. These active functional groups initiate the chemical bonding between these moieties, which is mostly a hydrogen bond. The broad band of the formula at 3420 cm-1 supported this suggestion.

Energy dispersive X-ray spectroscopy (EDX) provides quantitative and qualitative data about the chemical composition of a sample through interactions between X-rays and the elements present. Fig. 3b shows the EDX spectrum of the prepared INS-CN/DP nano-formula. The spectrum revealed the presence of C, O, N, S and P elements in varying percentages, confirming the incorporation of all components in the nano-formula. EDX mapping images (Fig. 3c) illustrate the spatial distribution of each detected element within the nano-formula matrix.

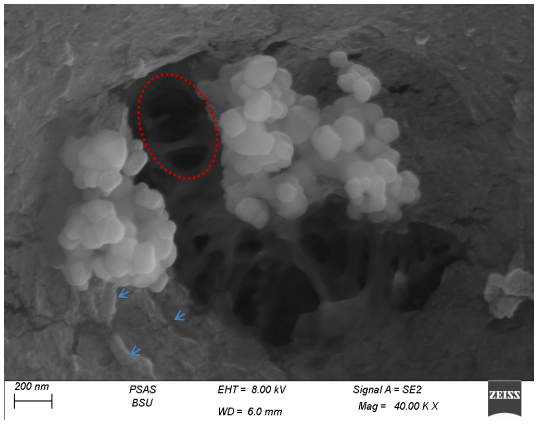


*(a)*

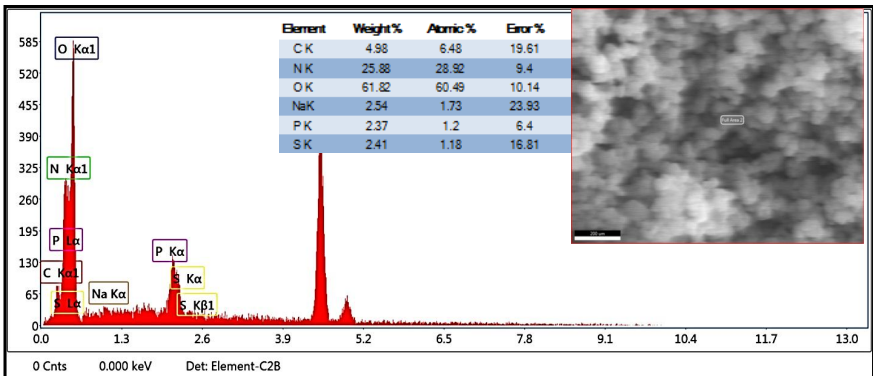


*(b)*

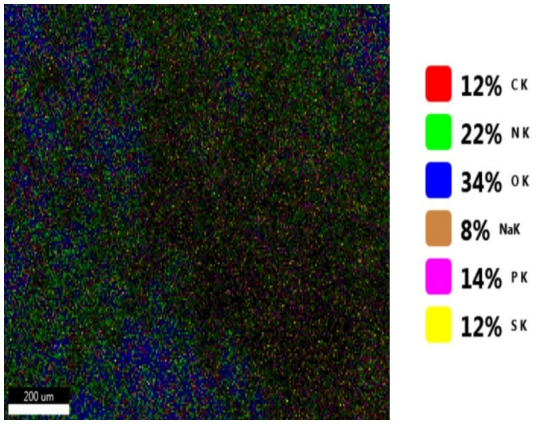


*(c)*

*Fig.3. SEM images of the prepared INS-CN/DP nanoparticles (a), the EDX spectra of the prepared formula (b), and the mapping images show the spatial distribution of each element in the formula (c).*

### 3.2. Zetasizer and Zeta potential measurements

Fig. 4 displays the hydrodynamic size distribution profile of the INS-CN/DP nanoparticles measured by dynamic light scattering. The mean hydrodynamic diameter of the nano-formula was determined to be 282.8 nm with a polydispersity index (PDI) of 0.106. The broad width of the distribution peak indicates a heterogeneous population with varying nanoparticle sizes. The intercept value of 0.819 signifies an adequate signal-to-noise ratio.

Using the zeta potential method, we measured the surface charge of the prepared formula. The value zeta potential were considered standard if it is more 30 mV, this value give ample repulsion force to reduce the aggregation of nanoparticles [26]. The measured value of zeta

potential was -16 mV, which reflects minimal physical stability and increases the interactions between the moieties either by chemical or electrostatic interaction. This was confirmed by the aggregated particles in the SEM image. The negative charge of the formula could be attributed to the hydroxy groups of pectin and dextrin and the carboxylic group of insulin, indicating the successful synthesis of the formula.

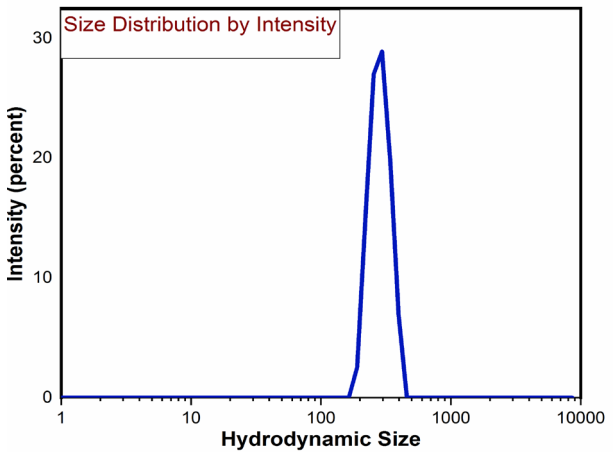


*Fig. 4. The hydrodynamic size and size distribution reported by the intensity of the prepared INS-CN/DP nanoparticles. The spectrum predicted a wide width of the distribution peak, indicating a heterogeneous size distribution.*

### 3.3. *In Vitro* Entrapment Efficiency, Release Profiles, and Kinetic Study

Based on the loading and encapsulation efficiency equations, the average LC% and EE% of insulin in the INS-CN/DP nanoparticles were 26.2 ± 0.56% and 69.3±2.75% respectively. Fig. 5 shows the cumulative percentage release of free and loaded insulin from the nano-formulation over 24 hrs in PBS at 37°C and pH 6.8. After 1 hr, loaded insulin release was ~10% versus 38% for free insulin. At 4 hrs, loaded release was 25% versus 48% for free. Loaded release gradually reached 63% at 8 hrs. The initial fast release is likely from surface-bound insulin. Slow release later is attributed to chitosan's poor solubility at pH 7.4, causing slower matrix swelling and erosion. Interactions between insulin and dextrin via hydrogen bonding also extend release time.

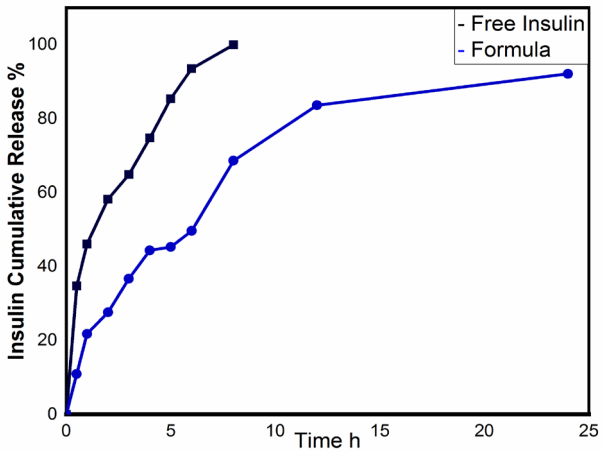


*Fig. 5. In vitro release profile of free insulin and INS-CN/DP nanoparticles for 24 h at pH 7.4 and 37°C. Results are mean ± SEM (n=3). The cumulative percentage release of the entrapped insulin increased in a gradual and slow pattern if compared to free insulin.*

Release kinetics analysis was performed to determine the release mechanism of insulin from the INS-CN/DP nanoparticles. The in vitro release data was fitted to five kinetic models - zero-order, first-order, Korsmeyer-Peppas, Hixson-Crowell and Higuchi equations (Fig. 6). Among these, Higuchi model showed the highest correlation coefficient (R2) value, followed by first-order and Hixson-Crowell models. This indicates that diffusion is the predominant mechanism governing insulin release from the nano-formulation. The good fit to Higuchi model suggests release is driven by Fickian diffusion. While first-order and Hixson-Crowell indicate the release is dependent on concentration gradient and surface erosion respectively.

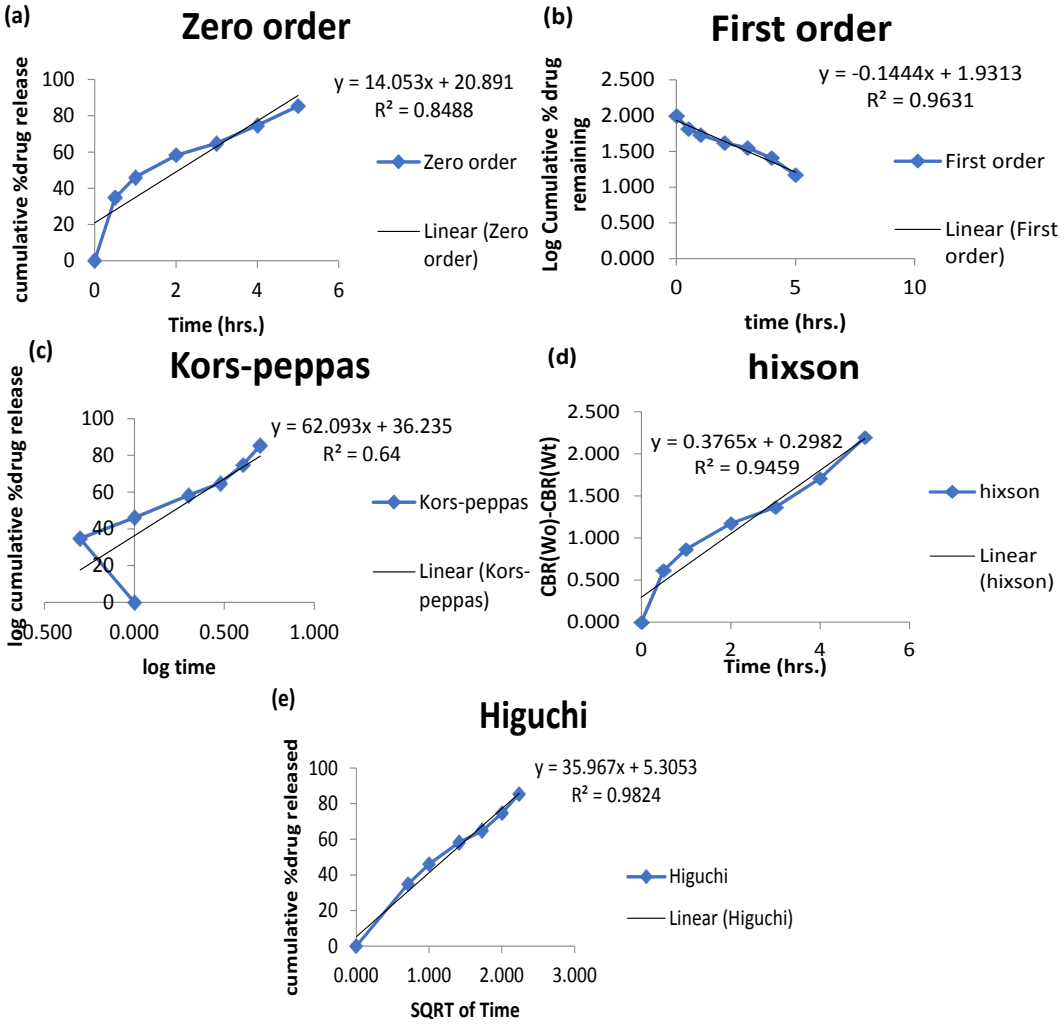


*Fig. 6. In vitro release kinetic study of the entrapped insulin in INS-CN/DP nanoparticles. The kinetic insulin release data were fitted using five equations: Zero-order equation (a), First-order equation (b), Korsmeyer-Peppas (c), Hixson-Crowell (d), and Higuchi (e). Insulin was highly best fitted to Higuchi.*

### 3.4. Effect of INS-CN/DP Nanoparticles on fasting and postprandial blood glucose

To follow up on the hypoglycemic efficiency of the INS-CN/DP nano-formula, fasting blood glucose (FBG) and postprandial blood glucose (PPBG) were investigated and depicted in Fig. 7. It was noted that the FBG and PPBG of diabetic control rats were highly elevated ($P<0.001$) in comparing to control normal ones. These outputs are in accordance with the previously published data confirming the stability of hyperglycemia in the streptozotocin diabetic rat model [27], [28]. This model is characterised by insulin deficiency that induces uncontrolled hepatic gluconeogenesis and glycogenolysis, disturbing glucose homeostasis and producing hyperglycemia [29], [30]. Treatment of diabetic rats with INS-CN/DP nanoparticles revealed a

significant (P<0.001) decline in FBG and PPBG when compared to those of diabetic control ones. In agreement with these findings, orally delivered insulin-loaded alginate and chitosan nanoparticles (50 and 100 IU/kg) in diabetic rats reduced serum glucose readings by more than 40%, whereas the hypoglycemic action was prolonged over 18 hours [31]. In comparison with the unloaded insulin treated group, the INS-CN/DP-treated group showed more powerful (P<0.001 and P<0.01, for FBG and PPBG, respectively) hypoglycemic action that may be interpreted by improved insulin bioavailability.

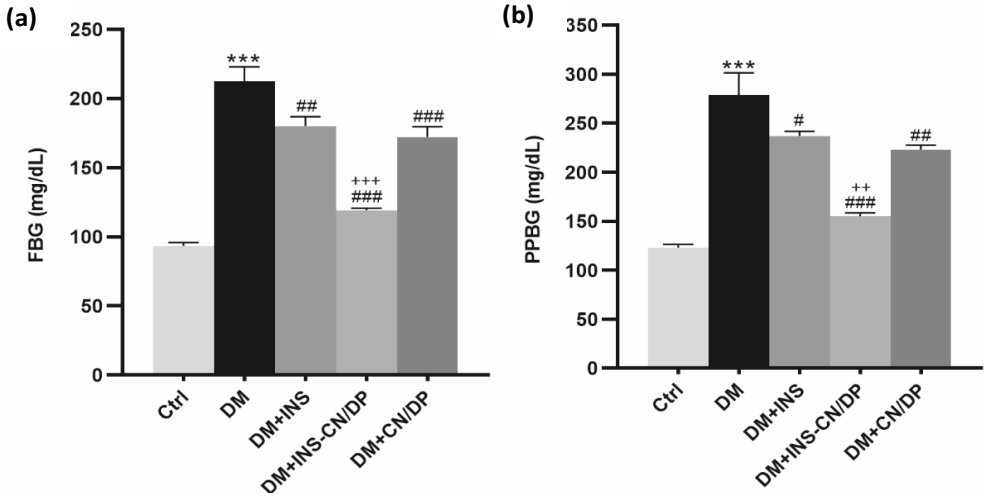


*Fig. 7. Effect of INS-CN/DP nanoparticles on the levels of (a) FBG, and (b) PPBG. Results are mean± standard error of the mean (n=6). $^{***}P$ <0.001 versus Ctrl; $^{\#}P$ <0.05, $^{\#\#}P$ <0.01 and $^{\#\#\#}P$ <0.001 versus DM; $^{++}P$ <0.01 and $^{+++}P$ <0.001 versus DM+INS. FBG, Fasting blood glucose; PPBG, Postprandial blood glucose.*

Furthermore, we noticed that diabetic rats treated with blank CN/DP nanoparticles revealed a significant hypoglycemic effect compared to diabetic control ones. These findings explained by the previous studies that reported the hypoglycemic action of nanoparticle-forming polymers. The consumption of chitosan oligosaccharide can efficiently decline postprandial blood glucose [9]. Wicker *et al.* [32] reported that pectin showed hypoglycemic activity mainly because it reduces glucose absorption. The anti-diabetic action of pectin may also be explained through modulation of the PI3K/Akt signalling pathway [11]. In the same line, dextrin has been reported to reduce postprandial blood glucose in both healthy subjects and type 2 diabetic patients [33].

### 3.5. Effect of INS-CN/DP Nanoparticles on Carbohydrate Metabolizing Enzymes

One of the major reflections of defects in carbohydrate hemostasis is the alterations in the activity of carbohydrate metabolism-related enzymes. Pyruvate kinase (PK) is key enzyme during glucose decomposition and catalyzes the conversion of phosphoenolpyruvate to pyruvate with the generation of ATP [34], [35]. Succinate dehydrogenase (SDH) participates in the tricarboxylic acid cycle and glycolysis [36].

The activities of both PK and SDH in diabetic rats significantly (P<0.001) dropped relative to normal control rats. In line with this, PK and SDH activities were decreased because of insulin deficiency in diabetic rats [37], [38]. Treatment of diabetic rats with INS-CN/DP nanoparticles significantly increased the activities of serum PK and SDH compared with diabetic control rats or diabetic rats treated with unloaded insulin (Fig. 8a and b). Moreover, diabetic rats treated with CN/DP nanoparticles displayed marked improvement in the activities of both enzymes (PK and SDH) compared with diabetic control rats. These changes in PK and SDH activities refer to enhanced glucose utilization that may be due to improved insulin sensitivity by nanoparticle-forming polymers. Palou *et al.* [39] verified that insulin sensitivity in rats with metabolic disorders

was improved by apple pectin. Chitosan has also been proven to increase insulin sensitivity in obese patients [40].

Glucose-6-phosphate dehydrogenase (G6PD) converts G6P into 6-phosphoglucono-δ-lactone, this step is important to channel glucose into the pentose phosphate pathway [41], [42]. NADPH is primarily produced by G6PD, and variations in G6PD activity will alter NADPH levels and thus affect the antioxidant system because NADPH regenerates reduced glutathione (GSH) from oxidized disulfide form of glutathione (GSSG) [43], [44]. The activity of G6PD in diabetic rats significantly ($P<0.001$) dropped relative to normal control rats. These results are in line with those of Abd El-Hameed *et al.* [38]. Decreased G6PD function led to lower intracellular NADPH concentrations, greater intracellular ROS, and increased oxidative stress levels [45]. Treatment of diabetic rats with INS-CN/DP nanoparticles significantly ($P<0.001$) elevated the activity of G6PD compared with diabetic control rats. INS-treated diabetic rats displayed a non-significant ($P>0.05$) change in G6PD activity, while INS-CN/DP nanoparticle-treated rats revealed a significant ($P<0.05$) increase compared to the INS-treated group (Fig. 8c). As predicted, the activity of this essential enzyme was noticeably elevated following administration of the insulin nano-formula, which may be due to improvements in insulin bioavailability and action.

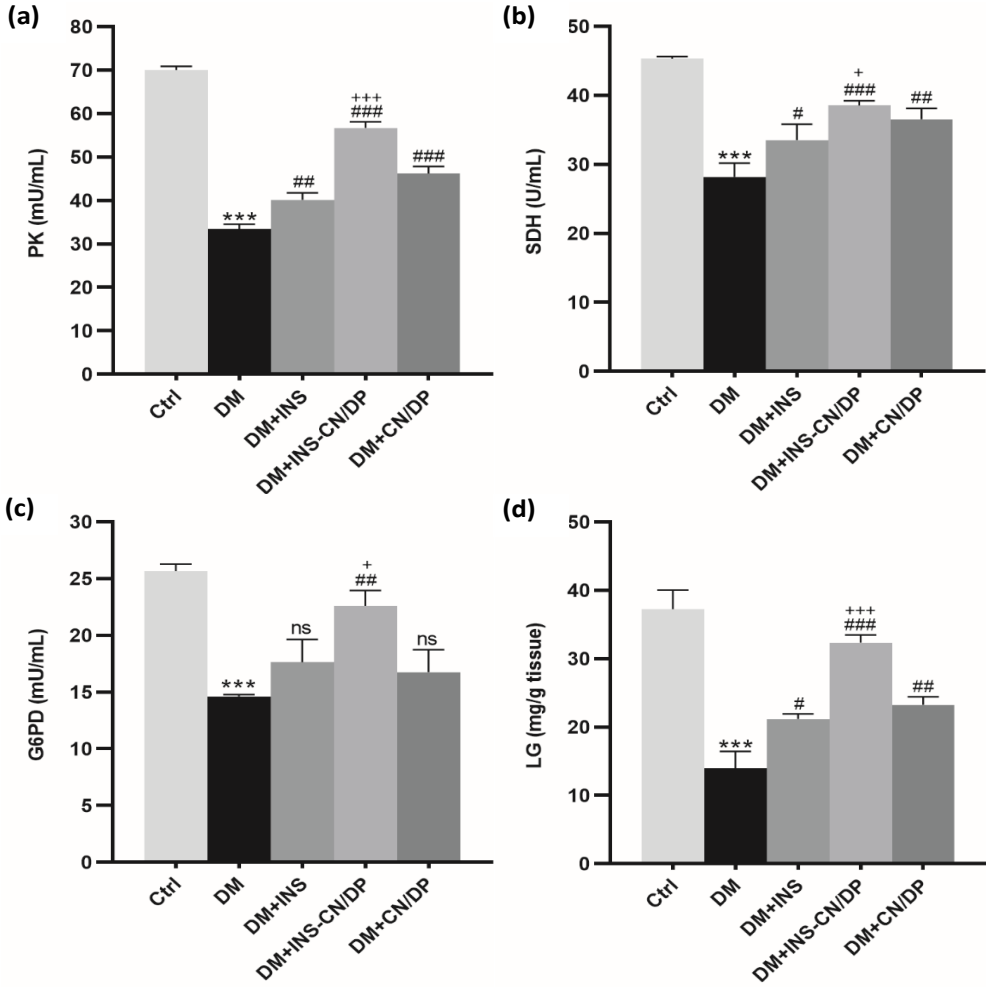


*Fig. 8. Effect of INS-CN/DP nanoparticles on the activites of (a) SDH, (b) PK, and (c) G6PD as well (d) LG. Results are mean± standard error of the mean (n=6). $^{***}P<0.001$ versus Ctrl; $^{ns}P\geq0.05$, $^{\#}P<0.05$, $^{\#\#}P<0.01$ and $^{\#\#\#}P<0.001$ versus DM; $^{+}P<0.01$ and $^{+++}P<0.001$ versus DM+INS. SDH, Succinate dehydrogenase; PK, Pyruvate kinase; G6PD, Glucose-6-phosphate dehydrogenase; LG, Liver glycogen.*

### 3.6. Effect of INS-CN/DP Nanoparticles on Hepatic Glycogen Content

Glycogen content is a directly linked to insulin activity in which insulin activates glycogen synthase, thus promotes glycogen deposition [46]. While, lack of insulin activates the glycogenolytic pathway, and the amount of stored glycogen decreases [47]. Liver glycogen content in the diabetic control rats displayed an obvious ($P<0.001$) decline as compared to that of normal control rats, as illustrated in Fig. 8d. Upon treatment with INS-CN/DP nanoparticles, liver glycogen content was significantly ($P<0.001$) restored. INS-CN/DP nanoparticles revealed a powerful restoring effect on liver glycogen as compared to unloaded insulin. Diabetic rats treated with blank CN/DP nanoparticles also showed obvious restoration of glycogen content. In concomitance, Liu *et al.* [11] stated that pectin administration improved glucose intolerance and glycogen level in the liver of diabetic rats.

### 3.7. Effect of INS-CN/DP Nanoparticles on GK and GULT-2 mRNA Expression

Hepatic glucokinase (GK) is recognized as a physiological indicator of glucose and catalyzes the phosphorylation of glucose to glucose 6-phosphate (G6P) [48], [49]. In diabetics, GK gene expression in liver is downregulated as it found that GK expression is related to insulin deficiency [50]. Glucose transporter-2 (GLUT-2) is the principal carrier for delivering plasma glucose into hepatocytes which is translocated from the cytoplasm to the plasma membrane due to elevated levels of plasma glucose [51]. When it comes to type 2 diabetes, impaired GLUT-2 has frequently been linked to glucose sensitivity [52].

As shown in Fig. 9a &b, our results revealed that GK and GLUT-2 gene expression were markedly dropped ($P<0.001$) in diabetic groups compared to normal groups. These results agree with the study of Haeusler *et al.* [53] and Abd El-Hameed *et al.* [38] who stated that hepatic GK and GLUT-2 expression obviously downregulated under diabetic conditions. Oral administration of INS-CN/DP nanoparticles to diabetic rats significantly ($P<0.001$) elevated GK and GLUT-2 gene expression levels compared with diabetic control rats. Notably, INS-CN/DP nanoparticles treated diabetic rats also revealed a significant ($P<0.001$) increase of GK expression in comparing to INS treated group. In line, it was stated that insulin induces GK expression in primary hepatocytes regardless of glucose concentration [54]. Therefore, restoring the Hepatic GK overexpression reduced glucose levels, whereas GK deficiency in mice was linked to hyperglycemia [55]. The improvement in GK and GLUT-2 expression could be explained by high insulin bioavailability and action of INS-CN/DP nanoparticles.

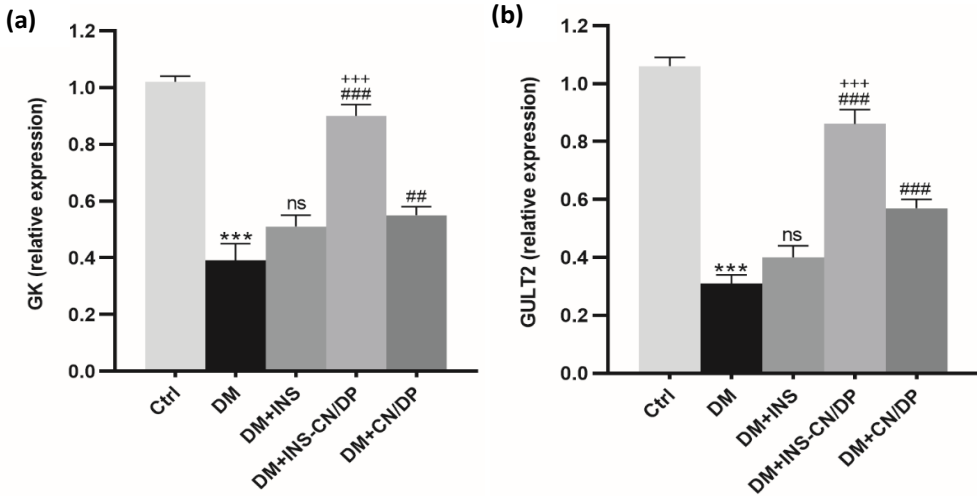


*Fig.9. Effect of INS-CN/DP nanoparticles on the gene expression levels of (a) GK, and (b) GULT2. Results are mean± standard error of the mean (n=6). $^{***}P<0.001$ versus Ctrl; $^{ns}P \geq 0.05$, $^{\#\#}P<0.01$ and $^{\#\#\#}P<0.001$ versus DM; $^{+++}P<0.001$ versus DM+INS. GK, Glucokinase; GULT2, Glucose transporter-2.*

## 4. Conclusion

To sum up, we assumed that our de novo-prepared oral INS-CN/DP nanoparticles were likely to show more effective hypoglycemic and antidiabetic efficiency compared to free insulin. This deduction could basically be connected to high insulin bioavailability alongside the antidiabetic actions of nanoparticle-forming polymers (chitosan, dextrin, and pectin), such as improving insulin sensitivity, modulating glucose metabolic pathways, inhibiting glucose absorption, and reducing postprandial blood glucose. INS-CN/DP nanoparticles seemed to be promising oral insulin delivery system and can act as a potential convenient alternative for insulin injections in diabetic patients after further clinical studies.

**Acknowledgments**

The authors are thankful to all members at Materials Science and nanotechnology Department, Faculty of Postgraduate Studies for Advanced Sciences (PSAS), Beni-Suef University for supporting preparation and characterization of the nanomaterials and all members of Animal House at Zoology Department, Faculty of Science, Beni-Suef University, Beni-Suef, Egypt for supporting *in vivo* study.

## References

[1] F. Bahman, K. Greish, S. Taurin, Pharmaceutical nanotechnology, 7, 2, 113-128 (2019); https://doi.org/10.2174/2211738507666190321110721

[2] E. Choi et al., Scientific Reports,13, 1, 11725 (2023); https://doi.org/10.1038/s41598-023-29106-w

[3] M. S. Alai, W. J. Lin, S. S. Pingale, Journal of food and drug analysis, 23, 3, 351-358 (2015); https://doi.org/10.1016/j.jfda.2015.01.007

[4] K. Ji et al., Med-x, 1, 1, 7 (2023).

[5] N. A. Peppas, N. J. Kavimandan, European Journal of Pharmaceutical Sciences, 29, 3-4, 183-197 (2006); https://doi.org/10.1016/j.ejps.2006.04.014

[6] M. J. Ansari, Journal of Medical Sciences, 15, 5, 209 (2015); https://doi.org/10.3923/jms.2015.209.220

[7] Y. Pan et al., International Journal of Pharmaceutics, 249, 1-2, 139-147 (2002); https://doi.org/10.1016/S0378-5173(02)00486-6

[8] A. Qiu, Y. Wang, G. Zhang, H. Wang, Polymers, 14, 15, 3217 (2022); https://doi.org/10.3390/polym14153217

[9] S. Jeong, J. Min Cho, Y.-I. Kwon, S.-C. Kim, D. Yeob Shin, J. Ho Lee, Nutrition & Diabetes, 9, 1, 31 (2019); https://doi.org/10.1038/s41387-019-0099-4

[10] C.-Y. Chiu, I.-L. Chan, T.-H. Yang, S.-H. Liu, M.-T. Chiang, Journal of agricultural and food chemistry, 63, 11, 2979-2988 (2015); https://doi.org/10.1021/acs.jafc.5b00198

[11] Y. Liu, M. Dong, Z. Yang, S. Pan, International Journal of Biological Macromolecules, 89, 484-488 (2016); https://doi.org/10.1016/j.ijbiomac.2016.05.015

[12] C. E. Kozmus et al., Molecular nutrition & food research, 55, 11, 1735-1739 (2011); https://doi.org/10.1002/mnfr.201100287

[13] N. Thotakura, L. Kaushik, V. Kumar, S. Preet, P. V. Babu, Current pharmaceutical design, 24, 43, 5147-5163 (2018); https://doi.org/10.2174/1381612825666190206211458

[14] K. Nagpal, S. K. Singh, D. N. Mishra, International Journal of Biological Macromolecules, 59, 72-83 (2013); https://doi.org/10.1016/j.ijbiomac.2013.04.024

[15] T. H. H. Gatti et al., Brazilian Journal of Pharmaceutical Sciences, 54 (2018).

[16] L. N. Ribeiro, A. C. Alcântara, M. Darder, P. Aranda, F. M. Araújo-Moreira, E. Ruiz-Hitzky,

International journal of pharmaceutics, 463, 1, 1-9 (2014); https://doi.org/10.1016/j.ijpharm.2013.12.035
[17] O. A. Ghosheh, A. A. Houdi, P. A. Crooks, Journal of pharmaceutical and biomedical analysis, 19, 5, 757-762 (1999); https://doi.org/10.1016/S0731-7085(98)00300-8
[18] N. Tamilselvan, C. V. Raghavan, Journal of young pharmacists, 7, 1, 28 (2015); https://doi.org/10.5530/jyp.2015.1.6
[19] N. Mhlanga, S. S. Ray, International journal of biological macromolecules, 72, 1301-1307 (2015); https://doi.org/10.1016/j.ijbiomac.2014.10.038
[20] F. G. Soufi, M. Vardyani, R. Sheervalilou, M. Mohammadi, M. H. Somi, Gen Physiol Biophys, 31, 4, 431-438 (2012); https://doi.org/10.4149/gpb_2012_039
[21] S. Dhanasekaran, P. Rameshthangam, S. Venkatesan, S. K. Singh, S. R. Vijayan, Journal of Polymers and the Environment, 26, 4095-4113 (2018); https://doi.org/10.1007/s10924-018-1282-8
[22] A. Hosni, A. Abdel-Moneim, M. Hussien, M. I. Zanaty, Z. E. Eldin, A. A. El-Shahawy, International Journal of Biological Macromolecules, 221, 1415-1427 (2022); https://doi.org/10.1016/j.ijbiomac.2022.09.048
[23] E. E. Mohamed, A. Abdel-Moneim, O. M. Ahmed, K. M. Zoheir, Z. E. Eldin, A. A. El-Shahawy, Journal of Drug Delivery Science and Technology, 75, 103677 (2022); https://doi.org/10.1016/j.jddst.2022.103677
[24] D. Demir, S. Ceylan, D. Göktürk, N. Bölgen, Polymer Bulletin, 78, 2211-2226 (2021); https://doi.org/10.1007/s00289-020-03208-1
[25] D. N. A. Zaidel, N. N. Zainudin, Y. M. M. Jusoh, I. I. Muhamad, Journal of Engineering Science and Technology, 10, 3, 22-29 (2015).
[26] R. Tantra, P. Schulze, P. Quincey, Particuology, 8, 3, 279-285 (2010); https://doi.org/10.1016/j.partic.2010.01.003
[27] V. K. Bayrasheva et al., Journal of diabetes research, 2016 (2016). pages
[28] A. M. Ali et al., Oxidative medicine and cellular longevity, 2020 (2020); https://doi.org/10.1155/2020/1727142
[29] R. Marinho, R. A. Mekary, V. R. Muñoz, R. J. Gomes, J. R. Pauli, L. P. de Moura, Diabetology & Metabolic Syndrome, 7, 1-7 (2015); https://doi.org/10.1186/s13098-015-0064-x
[30] A. K. Rines, K. Sharabi, C. D. Tavares, P. Puigserver, Nature reviews Drug discovery, 15, 11, 786-804 (2016); https://doi.org/10.1038/nrd.2016.151
[31] B. Sarmento, A. Ribeiro, F. Veiga, P. Sampaio, R. Neufeld, D. Ferreira, Pharmaceutical research, 24, 2198-2206 (2007); https://doi.org/10.1007/s11095-007-9367-4
[32] L. Wicker, Y. Kim, M.-J. Kim, B. Thirkield, Z. Lin, J. Jung, Food Hydrocolloids, 42, 251-259 (2014); https://doi.org/10.1016/j.foodhyd.2014.01.002
[33] J. L. Slavin, V. Savarino, A. Paredes-Diaz, and G. Fotopoulos, Journal of International Medical Research, 37, 1, 1-17 (2009); https://doi.org/10.1177/147323000903700101
[34] V. Gupta, R. N. Bamezai, Protein science, 19, 11, 2031-2044 (2010); https://doi.org/10.1002/pro.505
[35] C.-L. He et al., Scientific reports, 6, 1, 21524 (2016).
[36] A. Edalat et al., Diabetologia, 58, 1532-1541 (2015); https://doi.org/10.1007/s00125-015-3577-9
[37] S. RajeswaraReddy, L. Thopireddy, N. Ganapathi, R. Kesireddy Sathyavelu, IJPR-Iranian Journal of Pharmaceutical Research, 11, 1, 277-286 (2012).
[38] A. M. Abd El-Hameed, A. I. Yousef, S. M. Abd El-Twab, A. A. El-Shahawy, A. Abdel-Moneim, Biochemistry (Moscow), 86, 179-189 (2021); https://doi.org/10.1134/S0006297921020061
[39] M. Palou, J. Sánchez, F. García-Carrizo, A. Palou, C. Picó, Molecular nutrition & food research, 59, 10, 2022-2033 (2015); https://doi.org/10.1002/mnfr.201500292
[40] S. O. Hernández-González, M. González-Ortiz, E. Martínez-Abundis, J. A. Robles-Cervantes,

Nutrition research, 30, 6, 392-395 (2010); https://doi.org/10.1016/j.nutres.2010.06.005
[41] R. F. Kletzien, P. K. Harris, L. A. Foellmi, The FASEB Journal, 8, 2, 174-181 (1994); https://doi.org/10.1096/fasebj.8.2.8119488
[42] A. Stincone et al., Biological Reviews, 90, 3, 927-963 (2015); https://doi.org/10.1111/brv.12140
[43] A. Salvador, M. A. Savageau, Proceedings of the National Academy of Sciences, 100, 24, 14463-14468 (2003); https://doi.org/10.1073/pnas.2335687100
[44] P. Diaz-Vivancos, A. de Simone, G. Kiddle, C. H. Foyer, Free Radical Biology and Medicine, 89, 1154-1164 (2015); https://doi.org/10.1016/j.freeradbiomed.2015.09.023
[45] V. Chevallier, M. R. Andersen, L. Malphettes, Biotechnology and bioengineering, 117, 4, 1172-1186 (2020); https://doi.org/10.1002/bit.27247
[46] V. Vats, S. P. Yadav, J. K. Grover, Journal of ethnopharmacology, 90, 1, 155-160 (2004); https://doi.org/10.1016/j.jep.2003.09.034
[47] R. Ramith et al., Food and Function, 7, 9, 3999-4011 (2016); https://doi.org/10.1039/C6FO00343E
[48] R. Dentin et al., Journal of Biological Chemistry, 279, 19, 20314-20326 (2004); https://doi.org/10.1074/jbc.M312475200
[49] M. Pozo, M. Claret, Trends in Endocrinology & Metabolism, 29, 8, 581-594 (2018); https://doi.org/10.1016/j.tem.2018.05.001
[50] I. Roncero et al., PloS one, 8, 4, e58797 (2013); https://doi.org/10.1371/journal.pone.0058797
[51] J. W. Baynes, M. Maeda, Medical Biochemistry E-Book, 34 (2018).
[52] Z.-Q. Ren et al., Nutrition, 31, 5, 733-739 (20150; https://doi.org/10.1016/j.nut.2014.10.012
[53] R. A. Haeusler, S. Camastra, B. Astiarraga, M. Nannipieri, M. Anselmino, E. Ferrannini, Molecular metabolism, 4, 3, 222-226 (2015); https://doi.org/10.1016/j.molmet.2014.12.007
[54] P. B. Iynedjian, D. Jotterand, T. Nouspikel, M. Asfari, P. R. Pilot, Journal of Biological Chemistry, 264, 36, 21824-21829 (1989); https://doi.org/10.1016/S0021-9258(20)88258-1
[55] H. Watanabe et al., Nature communications, 9, 1, 30 (2018).